

# The Glasma and the PHENIX Photons and Dileptons

Mickey Chiu<sup>(1)</sup>, Thomas K. Hemmick<sup>(2)</sup>, Vladimir Khachatryan<sup>(2)</sup>, Andrey Leonidov<sup>(3)</sup>,  
Jinfeng Liao<sup>(4,5)</sup>, Larry McLerran<sup>(1,5)</sup>

February 17, 2012

1. Physics Department, Bldg. 510A, Brookhaven National Laboratory, Upton, NY 11973, USA
2. Physics Department, Stony Brook University, Stony Brook, NY 11794-3800, USA
3. Lebedev Physical Institute, Leninsky Pr. 53, 119991 Moscow, Russia
4. Physics Department and Center for Exploration of Energy and Matter, Indiana University, 2401 N Milo B. Sampson Lane, Bloomington, IN 47408, USA
5. RIKEN BNL Research Center, Bldg. 510A, Brookhaven National Laboratory, Upton, NY 11973, USA

## Abstract

We discuss the PHENIX photon and dilepton data in the context of the Glasma. We find that the distributions of such electromagnetic production, while previously not well understood, might now be qualitatively and semi-quantitatively described after including the essential contribution arising from a thermalizing Glasma. In particular, the  $p_T$  dependence of the low mass di-lepton excess as measured by PHENIX may be consistent with production from a transient Bose-Einstein condensate of gluons in the pre-equilibrium matter.

## 1 Introduction

Two traditional probes of matter produced in heavy ion collisions are photons and dileptons[1]-[4]. Photons and dileptons, while produced since very early times in the collisions, propagate through the produced matter largely without interaction. This is because of small electromagnetic cross sections.

The PHENIX experimental collaboration has looked for such photons and dileptons in collisions at RHIC and have reported surprising results [5]-[6]. There is a large excess of photons in the transverse momentum range of  $1-3 \text{ GeV}$  for central gold-gold collisions. This excess far exceeds that due to direct photons and has been interpreted by the PHENIX collaboration to represent photons produced by a Quark Gluon Plasma with a temperature in excess of that of the deconfinement temperature. They subsequently measured the flow of such photons and found it to be sizable and exceeding the expectation from the hydrodynamic expansion of a Quark Gluon Plasma [7]. The

PHENIX collaboration also measured an excess of dilepton pairs in the mass range  $100 \text{ MeV} \leq M \leq 1 \text{ GeV}$ . Hydrodynamic computations assuming a Quark Gluon plasma fail to reproduce the magnitude of this excess as well as the photon elliptic flow. In addition, the slope of the  $p_T$  distribution for such excess pairs is about  $100 \text{ MeV}$ , much less than the typical mass of the dilepton pairs. If such pairs arose either for a thermal emission from a Quark Gluon Plasma or from semi-hard processes, one would expect  $p_T \sim M$ .

It is tempting to assume that these photons and dileptons are associated with the energetic pre-equilibrium matter produced in early stages of heavy ion collisions. Such matter however does not appear to have the properties one would associate with a thermally equilibrated Quark Gluon Plasma. A logical question to ask is whether these probes have their origin in other more exotic forms of energetic matter. In a recent paper, it has been proposed that the Glasma, in early stages of a heavy ion collision, while strongly self interacting, might take a long time to thermalize, and during this pre-thermal stage might contain a Bose condensate of gluons [8]. The Glasma begins in the earliest stages of heavy ion collisions as an ensemble of longitudinal color electric and color magnetic lines of flux, and then decays into gluons with perhaps a transient Bose condensate also present[9]-[12]. The name Glasma is given because it is the matter in between that of the Color Glass Condensate and that of the thermally equilibrated Quark Gluon Plasma[13]. It can be thought of as a strongly interacting but not thermally equilibrated Quark-Gluon Plasma. It is strongly interacting due to coherence even though the coupling is weak

In this paper, we will make a very preliminary estimate of the electromagnetic emission properties of this Glasma. While our estimates are not as detailed as those for the Quark Gluon Plasma, we will find nevertheless, that the Glasma appears to have the correct qualitative and semi-quantitative features to explain the observed PHENIX photons and dileptons. In this paper a number of somewhat crude approximations will be made due to our currently incomplete knowledge of the Glasma, and as was the case for the Quark Gluon Plasma, more careful computation may reveal significant discrepancies with the PHENIX data.

Some of the aspects we need to describe the PHENIX data are not unique to the Glasma description. Guided by insight we have gotten from the Glasma treatment we will also discuss generic features needed for a description of the data at the end of this paper. Of course, the data concerning the di-leptons are controversial at the moment, and there have been alternative data presented by the STAR collaboration (albeit measured with different acceptance) [14] that are not in line with the strong excess found by PHENIX. While PHENIX measures yield into a different aperture than STAR and hence their superficially different results are not necessarily inconsistent, a final clarification on the experimental side is extremely important and may call for rethinking on various aspects of the Glasma treatment.

The paper is organized as follows: in the second section we will review those recently developed results for the Glasma which will be needed to estimate the photon and dilepton rates; in the third section, we will then use these results to derive the photon and dilepton rates, accounting for the time evolution of the Glasma; in the fourth section, we compare our results with the data from the PHENIX collaboration; finally in the last section, we will draw our conclusions and discuss various caveats and systematical improvements that can be done for our present estimations.

## 2 Review of Relevant Properties of the Thermalizing Glasma

In this section, we briefly review a recently proposed scenario for the thermalization process in the Glasma. The results relevant to our discussion of electromagnetic production will be presented, while all the details can be readily found in [8].

During the earliest stage of the evolution of the Glasma,  $0 \leq t \sim 1/Q_{sat}$  where  $Q_{sat}$  is the gluon saturation momentum, the gluonic degrees of freedom are largely coherent longitudinal color electric and color magnetic fields. Gluons, in the sense of particles, are being produced from the classical evolution of color electric and color magnetic fields, and these gluons produce a distribution that is approximately isotropic in momentum space, due to plasma instabilities. Not many quarks are present since they are produced by quantum fluctuations in the gluon field, and this is suppressed by a power of  $\alpha_s$ . The QCD coupling constant is small if the gluon saturation momentum is large compared to the QCD scale, which we shall assume.

We shall not discuss the photons and dileptons produced at this earliest time. Instead, we will concentrate on the time interval  $1/Q_{sat} \ll t \ll t_{therm}$  where  $t_{therm}$  is the thermalization time. During this time interval, the quark density increases to a value of the order of the gluon density, and is no longer suppressed. Since electromagnetic particle production ultimately arises from the electromagnetic charges of quarks, it is plausible that the production for  $t \sim 1/Q_{sat}$  might not be important. Further, we will concentrate on transverse momentum and mass scales where we expect that the effects of the evolution to a thermalized distribution are enhanced.

We assume the gluon density is of the form

$$f_g = \frac{\Lambda_s}{\alpha_s p} F_g(p/\Lambda) \quad (1)$$

In this equation,  $p$  is the gluon momentum.  $\Lambda_s$  is the momentum scale at which the gluons are maximally coherent and is time dependent. At the earliest times  $\Lambda_s(t_0) \sim Q_{sat}$ .  $\Lambda$  is a time dependent ultraviolet cutoff, which at the earliest time coincides with  $\Lambda_s$  i.e.  $\Lambda(t_0) = \Lambda_s(t_0)$ . The scale  $\Lambda$  however continuously separates from  $\Lambda_s$  during the course of thermalization, and upon equilibration becomes the initial temperature for the Quark-Gluon Plasma  $\Lambda(t_{therm}) \sim T_i$ . The soft scale  $\Lambda_s$ , on the other hand, becomes the non-perturbative “magnetic scale” [15] in the thermalized plasma  $\Lambda_s(t_{therm}) \sim \alpha_s T_i$ . The thermalization is therefore accomplished by splitting apart these initially overlapping momentum scales by  $\alpha_s$  parametrically, and the corresponding time is determined by the following requirement

$$\Lambda_s(t_{therm}) \sim \alpha_s \Lambda(t_{therm}) \quad (2)$$

To achieve such separation takes parametrically long time in the very high energy limit and could take considerable time even at the RHIC energy.

A very important consequence of the saturation is that the phase space for the gluons is initially over-occupied

$$n_g/\epsilon_g^{3/4} \sim 1/\alpha_s^{1/4} \quad (3)$$

where  $n_g$  is the number density of gluons, and  $\epsilon_g$  is the energy density in the gluons. For a thermally equilibrated Bose system, it is necessary that this ratio be less than a number of the order 1. It is therefore plausible that in addition to the gluons, a Bose-Einstein condensate could be developed with time by “absorbing” the large number of excessive gluons into zero momentum state (provided that the inelastic processes are not fast enough to sufficiently reduce the number of gluons prior to

thermalization). Such a condensate would be of the form

$$f_{cond} = n_{cond} \delta^3(p) \quad (4)$$

The condensate can be thought of as many gluons compressed into a color singlet and spin singlet configuration that are highly coherent and have zero momentum. We expect that the effective masses of the gluons in the condensate should be of the order of the Debye scale, which is

$$M_{Debye}^2 \sim \Lambda \Lambda_s \quad (5)$$

This is because when the condensate decays it must produce real time excitations and the minimum mass scale for such excitations is the Debye mass. The Debye mass will also act as an infrared cutoff in various dynamical processes.

It was shown in [8] that the time evolution is dominated by the gluon density, and that there may be some fixed asymmetry between the typical transverse and longitudinal momentum scales characterized by a parameter  $\delta$ . The parameter  $\delta$  is defined in terms of the longitudinal pressure

$$P_L = \delta \epsilon \quad (6)$$

where  $0 \leq \delta \leq 1/3$ , with  $\delta = 0$  and  $\delta = 1/3$  corresponding to the free-streaming (thus maximal anisotropy between the longitudinal and transverse pressure) and the isotropic expansion, respectively. The time evolution of the scales  $\Lambda_s$  and  $\Lambda$  were found to be

$$\Lambda_s \sim Q_s \left( \frac{t_0}{t} \right)^{(4+\delta)/7} \quad (7)$$

and

$$\Lambda \sim Q_s \left( \frac{t_0}{t} \right)^{(1+2\delta)/7} \quad (8)$$

This can be translated into the gluon density and the Debye mass as

$$n_g \sim \frac{Q_{sat}^3}{\alpha_s} \left( \frac{t_0}{t} \right)^{(6+5\delta)/7} \quad (9)$$

and

$$M_{Debye}^2 \sim Q_{sat}^2 \left( \frac{t_0}{t} \right)^{(5+3\delta)/7} \quad (10)$$

The thermalization time is given by

$$t_{therm} \sim t_0 \left( \frac{1}{\alpha_s} \right)^{7/(3-\delta)} \quad (11)$$

It is difficult to determine the time evolution of the gluon condensate density without fully addressing the inelastic processes. Nevertheless one may assume an approximation transport equation of the form

$$\frac{d}{dt} n_{cond} = -\frac{a}{t_{scat}} n_{cond} + \frac{b}{t_{scat}} n_g \quad (12)$$

Here  $t_{scat} \sim t$  is the universal scattering time for the Glasma and  $a$  and  $b$  are constants of order 1. The first term represents the decay of condensate due to inelastic processes, while the second term reflects the “feeding” into condensate from the over-occupied gluons. (This equation is for illustration shown for a non-expanding medium, but analogous results are easy to derive for an expanding medium.) Under the above approximation it can be deduced that either the condensate decreases more slowly than the gluon density if  $a < b$ , or the condensate density stays at the order of the gluon density if  $a \geq b$ . In either case one has  $n_{cond} \geq n_g$ , and for simplicity we will use the following assumption for later discussions:

$$n_{cond} = \kappa n_{gluon} \quad (13)$$

where  $\kappa$  is a constant of order 1.

Finally, to complete our description, we need the quark number density that is

$$f_q = F_q(p/\Lambda) \quad (14)$$

so that the quark number density is

$$n_q \sim \Lambda^3 \quad (15)$$

At the earliest times  $n_q \sim \alpha_s n_g \ll n_g$ , but at late time the two densities approach each other, i.e.  $n_q \sim n_g$ .

### 3 Electromagnetic Particle Production from the Glasma

Now let us first estimate the rate of photon production from the Glasma. Recall that the quark number density, up to an overall constant is identical to that for the quark number density in a Quark Gluon Plasma with the replacement  $\Lambda \rightarrow T$ . The computations of the rate for photon production at finite temperature are reviewed in Ref. [16]. For thermal emission from a Quark Gluon Plasma in a fixed box, the result is

$$\frac{dN}{d^4x dy d^2k_T} = \frac{\alpha \alpha_s}{2\pi^2} T^2 e^{-E/T} h(E/T) \quad (16)$$

where  $h$  is a slowly varying function of  $E/T$  of the order one. The factor of  $\alpha_s$  arises from the interaction of quarks with the medium in the photon production process. (This formula and the ones that follow are evaluated in the local rest frame of the fluid, and require generalization for use in a boosted frame.)

In the Glasma, this is compensated for by the high gluon density  $\sim 1/\alpha_s$  associated with the coherence of the Glasma. For Glasma emission, we shall use a simplified form of this equation,

$$\frac{dN}{d^4x dy d^2k_T} = \frac{\alpha}{\pi} \Lambda_s \Lambda g(E/\Lambda) \quad (17)$$

Here,  $g$  is a function of order one that cuts off when the energy of the photon is of the order of the UV cutoff scale  $\Lambda$ . This form follows from dimensional reasoning, and the fact that the overall rate must be proportional to the electromagnetic coupling. The factor of  $\Lambda$  is analogous to the temperature factor for thermal emissions. There is a factor of  $\Lambda_s/\alpha_s \Lambda$  relative to the naive generalized thermal formula. This factor arises because one of the external legs of the diagram that induces photon emissions couples to a coherent Glasma photon and this has a distribution function

proportional to  $\Lambda_s/\alpha_s$ . The factor of  $g(E/\Lambda)$  occurs because  $\Lambda$  is the largest momentum scale in the problem and quarks always have a typical momentum scale of order  $\Lambda$ . Whether the gluon arises from thermal gluons or from the gluon condensate is not important, since we will assume the density of gluons and the density of the condensate are the same. This will only affect the external line factors but not the dependence of  $g(E/\Lambda)$ , because it is the largest momentum scale, i.e. that of the quarks, that determines such dependence. Note that at thermalization when  $T \sim \Lambda \sim \Lambda_s/\alpha_s$ , this formula reduces to that for thermal emission.

To obtain the overall rate, we need to integrate over longitudinal coordinates. We assume that the early time expansion is purely longitudinal, and that in the integration the space-time rapidity is strongly correlated with that of the momentum space-rapidity. We then have that

$$\frac{dN}{d^2r_T dy d^2k_T} \sim \alpha \int t dt \Lambda_s \Lambda g(k_T/\Lambda) \quad (18)$$

Using the result of the previous section for the time dependence of the scales  $\Lambda$  and  $\Lambda_s$ , we have

$$t dt = \kappa' \frac{d\Lambda}{\Lambda} \frac{1}{Q_{sat}^2} \left( \frac{Q_{sat}}{\Lambda} \right)^{14/(1+2\delta)} \quad (19)$$

The constant  $\kappa'$  is of order 1.

Doing the integration over  $\Lambda$  in Eqn.(18), we find that

$$\frac{dN}{d^2r_T dy d^2k_T} \sim \alpha \left( \frac{Q_{sat}}{k_T} \right)^{\frac{9-3\delta}{1+2\delta}} \quad (20)$$

Now integrating over  $d^2r_T$ , and identifying the overlap cross section as proportional to the number of participants, we finally obtain

$$\frac{dN_\gamma}{dy d^2k_T} = \alpha R_0^2 N_{part}^{2/3} \left( \frac{Q_{sat}}{k_T} \right)^\eta \quad (21)$$

where  $\eta = (9 - 3\delta)/(1 + 2\delta)$ . The factor of  $N_{part}^{2/3}$  arises because the number of participants in a collision proportional to the nuclear volume  $R^3 \sim N_{part}$ . Here  $R_0$  is a constant with dimensions of a length. It should be of order 1 fm, but cannot be determined precisely due to the crude approximations made. The power of  $Q_{sat}/k_T$  ranges from

$$9 \geq \eta \geq 24/5 \quad (22)$$

with the two limits  $\eta = 9$  and  $\eta = 24/5$  corresponding to  $\delta = 0$  (maximal anisotropy) and  $\delta = 1/3$  (isotropic expansion) respectively. Note that in this formula, once the power of  $k_T$  has been determined from experiment, then using that  $Q_{sat}^2 \sim N_{part}^{1/3}$ , we have that the cross section scales as  $N_{part}^{2/3+\eta/6}$ . This is a very rapid dependence on the number of participants.

It is important to note that in the derivation of this result, we have assumed that the largest part of the contribution when integrating over  $\Lambda$  does not come from the end points of the integration. If the end points become important, then the physics either from the earliest times (hard processes) or from the thermalized Quark Gluon Plasma will become important. For the case of a Quark Gluon

Plasma, the dominant region of integration is  $k_T \sim 6T$ . The smallest possible value for  $\Lambda$  would be of the order of the QCD transition temperature, and at RHIC energies the highest possible value for  $\Lambda$  shall be around 1 GeV. These considerations are therefore valid at best for photon production in the range of  $1 \text{ GeV} \leq k_T \leq 10 \text{ GeV}$ .

The analysis of dilepton pair production is more complicated because there are two sources of di-leptons. The first is due to annihilation of quarks in the Glasma. For this contribution, the rate can be determined by dimensional reasoning to be

$$\frac{dN_{DY}}{d^4x dy dM^2} = \alpha^2 \Lambda^2 g'(M/\Lambda) \quad (23)$$

The evaluation of this contribution follows as above and gives

$$\frac{dN_{DY}}{dy dM^2} \sim \alpha^2 R_0'^2 N_{part}^{2/3} \left( \frac{Q_{sat}}{M} \right)^\eta \quad (24)$$

with  $\eta = 4(3 - \delta)/(1 + 2\delta)$  taking values  $12 \geq \eta \geq 32/5$  for  $0 \leq \delta \leq 1/3$ . Unfortunately, the derivation of this result requires very massive dileptons. Analogous to the limits on  $k_T$  for direct photon production, such contribution would be in the mass range greater than 1 GeV in which a variety of other processes such as charm particle decays would obscure a Drell-Yan signal. Also note that the most interesting “excess” seen in the RHIC data appears in the range between a few hundred MeV and about 1 GeV.

Let us however consider another process. This process is the annihilation of gluons into a quark loop from which the quarks then subsequently decay into a virtual photon and eventually the dilepton pair: see the illustration in the Fig.1. Such a virtual process is naively suppressed by factors of  $\alpha_s$ . Here however, the gluon arise from a highly coherent condensate, and the corresponding factors of  $\alpha_s$  are compensated by inverse factors  $1/\alpha_s$  from the coherence of the condensate. In other words, the usual power counting for diagrams in terms of  $\alpha_s$  has to be changed when the coherent condensate with high occupation is present.

This annihilation process from a condensate has a distinctive feature. The condensate gluons have nearly zero total momentum in a co-moving frame. All of the gluon momentum is acquired by collective flow, and hence the produced di-lepton pairs will have a small transverse momentum which could be much smaller compared with the pair mass. In contrast, for usual thermal production processes as well as hard particle production processes, the typical transverse momentum of the produced pair is of the order of the dilepton pair mass.

Here we estimate the rate for the three-gluon decay of the condensate into a diepton pair. On dimensional grounds, we expect that

$$\frac{dN_{C \rightarrow DY}}{d^4x dy dM^2} = \alpha^2 \frac{(\alpha_s n_{gluon})^3}{M_{Debye}^7} g''(M/M_{Debye}) \quad (25)$$

We are assuming the condensate density is of the order of the gluon number density as in Eq.(15). We are also assuming that the typical scale for the energy of gluons in the condensate is of order the Debye mass. It is also implicitly assumed that the condensate is unstable with respect to decay but gets stabilized by processes that build up the condensate due to the over-occupation of gluonic states. Note that in the scaling Glasma we have  $M_{Debye} \sim \sqrt{\Lambda \Lambda_s} \sim Q_s(t_0/t)^{(5+3\delta)/14}$ . Note that due to the external gluon lines, there is a correction to the result in Eq.(24) on the order of  $(\alpha_s n_{gluon})^3 / M_{debye}^9$ .

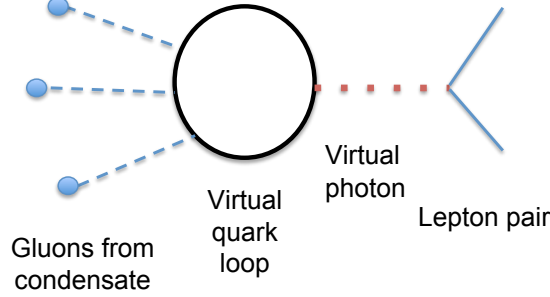


Figure 1: Three gluons from the condensate annihilate into a virtual quark loop, that subsequently decays into a virtual photon and then into a dilepton pair.

The coupling  $\alpha_s$  from each leg will be canceled by the high density  $1/\alpha_s$  from each leg and at the end one obtains an overall multiplicative factor  $(\alpha_s n_{gluon}/M_{debye}^3)^3 \sim (t/t_0)^{3(3-\delta)/14}$ . When the integration over time is concerted into that of factors of mass, we get the following result

$$\frac{dN_{C \rightarrow DY}}{dy dM^2} \sim \alpha^2 R_0'^2 N_{part}^{2/3} \left( \frac{Q_{sat}}{M} \right)^{\eta'} \quad (26)$$

where the exponent now becomes  $\eta'$  given by

$$\eta'_{perturbative} = \frac{9(3-\delta)}{5+3\delta} \quad (27)$$

It is valued in the range  $27/5 \geq \eta'_{perturbative} \geq 4$  corresponding to  $\delta = 0$  for maximal anisotropy and  $\delta = 1/3$  for isotropic expansion.

Because the time evolution of the Debye mass is much more rapid than is that for the ultra-violet cutoff scale  $\Lambda$ , we expect that the range where this formula applies is in a range of masses significantly smaller than is the case of the photons, and Drell-Yan emission for quarks. It is not unreasonable to expect that this formula works in the range somewhat below 1 GeV but may cut off at some small mass of order few hundred MeV. A detailed computation of the rate and determination of behavior near such a cutoff would be useful, since the cutoff is a measure of the temperature at which the condensate disappears, which is presumably the thermalization temperature.

The results we present above for three-gluon annihilation into a quark loop can and should be corrected for multiple gluon annihilation. For such soft gluon attachments, we believe these effects can, with some work, be analytically summed. Since more gluon attachments will increase the powers of time-dependence on the external legs, this will lead to a steepening of the dependence on the mass scale. The generic feature of geometrical scaling, that the distribution is a function of the form

$$\frac{dN_{C \rightarrow DY}}{dy dM^2} \sim \alpha^2 R_0'^2 N_{part}^{2/3} F_{DY}(Q_{sat}/M) \quad (28)$$

will not be modified, as this follows entirely from dimensional reasoning. The distribution from the condensate will also come from small momentum. We see that generic features of the distribution



that we wish to extract will remain, although the shape of the curve in  $M$  would have significant modification. As a practical matter, one needs to do the integration over the spacetime history much more accurately for the mass range seen at RHIC energies, since this range extends to rather low mass values.

We end by discussing a few theoretical issues in the above estimation. With the crude approximation above, we have estimated the contribution from one flavor of massless quark. The amplitude for this contribution is proportional to the quark charge. If we have multiple massless flavors, we have it proportional to  $\sum_i e_i$ . For the three light flavors  $u, d, s$ , this sum would vanish provided they are strictly degenerate in mass. A non-vanishing contribution would survive when the mass for the strange quark becomes relevant (e.g. when the scales are low), and/or a contribution from the charm quark becomes relevant (e.g. when the scales are high). Which contribution is dominant depends upon the scale of the di-lepton pair mass. These effects will generate an overall suppression and may introduce a non-trivial shape into the mass distribution. For example, the charm quark contribution could make the distribution harder i.e. less steep. Another concern is related to the spin states of the gluons in the condensate. The diagram in Fig.1 computes essentially the EM vector current correlator, and since the condensate gluons have zero spatial momentum the spatial structure will have to arise from the gluon spin indices. A nonzero contribution from the diagram is obtained if the gluon spin states are either incoherent and trivially averaged as is the case in thermal QGP (which we think shall be the case) or are coherently in a uniform spin orientation (thus breaking spatial isotropy). These issues would require further works for clarification.

## 4 Phenomenology of Photon and Di-lepton Emission

In this section we will present phenomenological formulae for electromagnetic emissions that follow from the theoretical results described in the previous sections, and compare the results with the experimental data on photons and di-leptons from the PHENIX collaboration.

### 4.1 Photons

We begin with Eq.(21) for the photon yield

$$\frac{dN_\gamma}{dy d^2k_T} \sim \alpha R_0^2 N_{part}^{2/3} \left( \frac{Q_{sat}}{k_T} \right)^\eta, \quad (29)$$

where  $\eta = (9 - 3\delta)/(1 + 2\delta)$ . The power of  $Q_{sat}/k_T$  ranges from  $9 \geq \eta \geq 24/5$  (corresponding to  $0 < \delta < 1/3$ , respectively). We use that

$$Q_{sat}^2(k_T/\sqrt{s}) = Q_0^2 \left( \frac{\sqrt{s} \times 10^{-3}}{k_T} \right)^\lambda, \quad (30)$$

where the  $\lambda$  is a parameter characterizing the growth of the saturation momentum with decreasing  $x$ . These lead to a result paralleling that of the analysis for  $pp$  scattering in Ref.[17]

$$\frac{dN_\gamma}{dy d^2k_T} \sim \alpha R_0^2 N_{part}^{2/3} \left( \frac{\sqrt{Q_0^2 (\sqrt{s} \times 10^{-3}/k_T)^\lambda}}{k_T} \right)^\eta \sim \alpha R_0^2 N_{part}^{2/3} \frac{\left( Q_0^2 (\sqrt{s} \times 10^{-3})^\lambda \right)^{\eta/2}}{k_T^{\eta(1+\lambda/2)}}. \quad (31)$$

Phenomenologically, one would expect a range  $0.2 \leq \lambda \leq 0.35$ . In this paper we will examine this wide range of parameter and find the best fitting results.

Based on the above, we will use the following phenomenological formulae for parameterizing the contribution from Glasma evolution to the photon production:

$$F(\lambda, \eta) \equiv C_\gamma N_{part}^{2/3} \times \frac{[Q_0^2 (\sqrt{s} \times 10^{-3})^\lambda]^{\eta/2}}{k_T^{\eta(1+\lambda/2)}}. \quad (32)$$

where the constant coefficient  $C_\gamma \propto \alpha R_0^2$  can be determined by fitting at one centrality bin and then applied to all other centralities. For comparison with data, one also needs to include the photon production from the initial  $pp$  collisions (without any medium effect). Such production can be described by properly scaled-up pQCD results for  $pp$  collisions. We use the Hagedorn function for parameterizing this “trivial” contribution:

$$G = T_{AA} \times \frac{A_{pp}}{(1 + k_T^2/b)^n} \quad (33)$$

where  $T_{AA}$  is the Glauber nuclear overlap function depending on centrality. This part of contribution is well studied with the parameters determined to be  $A_{pp} = 0.0133264 \text{ mb}$ ,  $b = 1.5251 \text{ GeV}^2$  and  $n = 3.24692$ . The phenomenological formula for total photon production will therefore be a sum of the two contributions  $F + G$ .

The data we aim to describe will be the invariant yield in  $Au$ - $Au$  collisions at  $\sqrt{S_{NN}} = 200 \text{ GeV}$  of direct photons at centralities 0-20%, 20-40% and 0-92.2% (Min. Bias) as a function of  $k_T$  from PHENIX measurement: see Fig.34 of Ref. [6]. The strategy is the following: for given values of  $\lambda$  and  $\eta$  in Eq.(32), we will fix the coefficient  $C_\gamma$  from the 0-20% case and test how well the formula describe the data at the other two centrality choices. This will provide a critical test of the geometric scaling properties of the present model.

We now discuss the various parameters involved in the comparison.

(1) For the key parameters  $\lambda$  and  $\eta$  in Eq.(32), we test a wide range of choices for  $0.2 \leq \lambda \leq 0.35$  and  $24/5 \leq \eta \leq 9$ . For each specification of  $\lambda$  and  $\eta$  values, we can do the fitting for photon data at all centralities and evaluate the corresponding  $\chi^2/\text{d.o.f.}$  which will allow us to find the regions of  $\lambda$  and  $\eta$  for the best fitting results.

(2) For  $N_{part}$  and  $T_{AA}$ , we use the Glauber model calculation from PHENIX for these centralities:  $\langle N_{part} \rangle = 279.9$  and  $T_{AA} = 18.55 \text{ mb}^{-1}$  at 0-20%;  $\langle N_{part} \rangle = 140.4$  and  $T_{AA} = 7.065 \text{ mb}^{-1}$  at 20-40%;  $\langle N_{part} \rangle = 109.1$  and  $T_{AA} = 6.14 \text{ mb}^{-1}$  at 0-92.2% (Min. Bias).

(3) For the saturation scale  $Q_0$  in Eq.(32), we determine its value at various centralities and beam energies by using the scaling properties  $Q_0^2 \propto N_{part}^{1/3}$  and  $Q_0^2 \propto (\sqrt{s})^{\lambda/(1+\lambda/2)}$  (see [18][19] for details), which gives the following values  $Q_0^2(0-20\%) = 1.895 \text{ GeV}^2$ ,  $Q_0^2(20-40\%) = 1.490 \text{ GeV}^2$ , and  $Q_0^2(0-92.2\%) = 1.384 \text{ GeV}^2$  to be used in our case.

Finally we present our fitting results for the PHENIX photon data. In Fig.2, we show the  $\chi^2/\text{d.o.f.}$  analysis in the  $\lambda - \eta$  parameter space for the PHENIX photon data in three centrality bins by plotting the three contours corresponding to 1- $\sigma$ (blue), 2- $\sigma$ (green), and 3- $\sigma$ (red) errors. Based on this analysis, one can identify a best-fitting zone (at about 2- $\sigma$  level) to be  $\lambda = 0.29 \pm 0.05$  and  $\eta = 6.65 \pm 0.60$  — the latter corresponding to the asymmetry parameter  $\delta = 0.144 \pm 0.045$ .

Having identified the optimal parameter regime, we now show in Fig.3 the direct comparison between data and our model fitting with  $\lambda = 0.29$  and  $\eta = 6.65 \pm 0.60$ . For each centrality bin, the

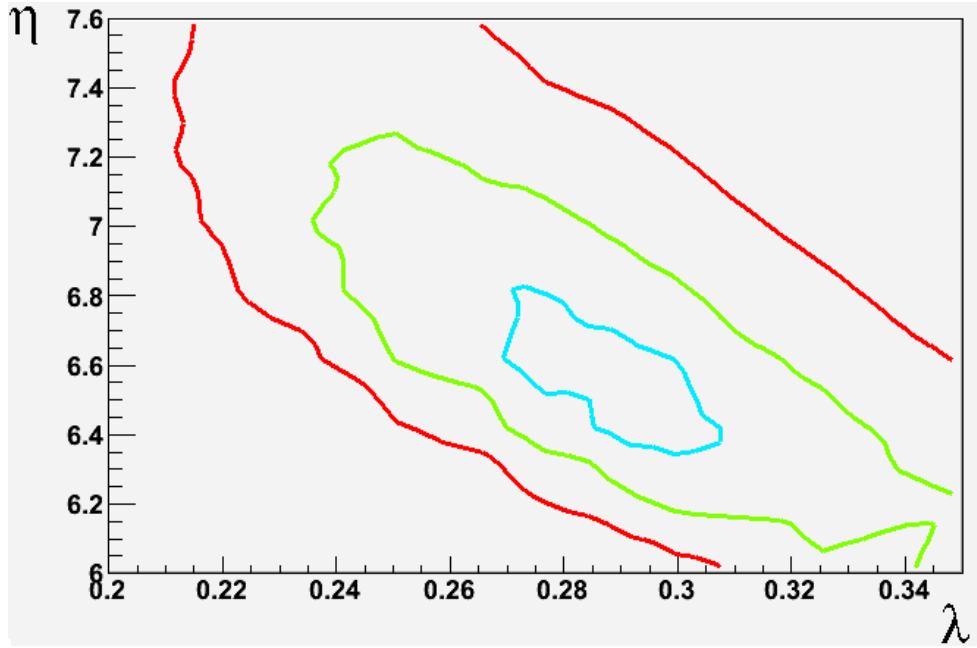


Figure 2: The  $\chi^2/\text{d.o.f.}$  analysis in the  $\lambda - \eta$  parameter space for the PHENIX photon data in three centrality bins by fitting with the present model, with the blue, green, and red contours indicating 1-, 2-, and 3- $\sigma$  errors, respectively (see text for more details).

PHENIX data points are compared with: (a) the contribution from only the  $T_{AA}$ -scaled pp yield, i.e. the Hagedorn function in Eq.(33), represented by the black dashed curves; and (b) the full yield including both the  $T_{AA}$ -scaled pp yield and the contribution from the Glasma in Eq.(32), represented by the colorful bands where the upper and lower boundary curves for each band correspond to the results with  $\eta = 6.65 - 0.60 = 6.05$  and  $\eta = 6.65 + 0.60 = 7.25$ , respectively. The plots show nice agreement between the PHENIX data and our model fitting at all centralities!

The only parameter directly determined from fitting is the overall normalization  $C_\gamma$  in Eq.(32): it has been fixed from the 0-20% case to be  $C_\gamma \approx 0.0234 \text{ fm}^2$  and then used in all other centralities. We notice that this value is consistent with the expectation  $C_\gamma \sim \alpha R_0^2$  provided  $\alpha = 1/137$ ,  $R_0$  of the order few fm and a reasonable coefficient.

A few remarks are in order from the comparison. First, while the very high  $k_T > 3 \text{ GeV}$  data are well described by the  $T_{AA}$ -scaled pp yield only, the inclusion of the Glasma contribution is necessary and even dominant for describing the “excess” in yield and the  $k_T$ -dependence in the softer region about  $1 \sim 3 \text{ GeV}$ . Second, the fact that data for varied centralities can be well fitted by one parameter  $C_\gamma$  fixed at one centrality provides strong evidence that our model for Glasma photon production has captured the essential geometrical scaling in such data in the relatively lower- $k_T$  region. Last, the comparison implies for the parameter  $\eta$  a preferred region  $\eta = 6.65 \pm 0.60$ , corresponding to a region  $\delta = 0.144 \pm 0.045$  for the asymmetric parameter  $\delta$  in Eq.(6) which appears

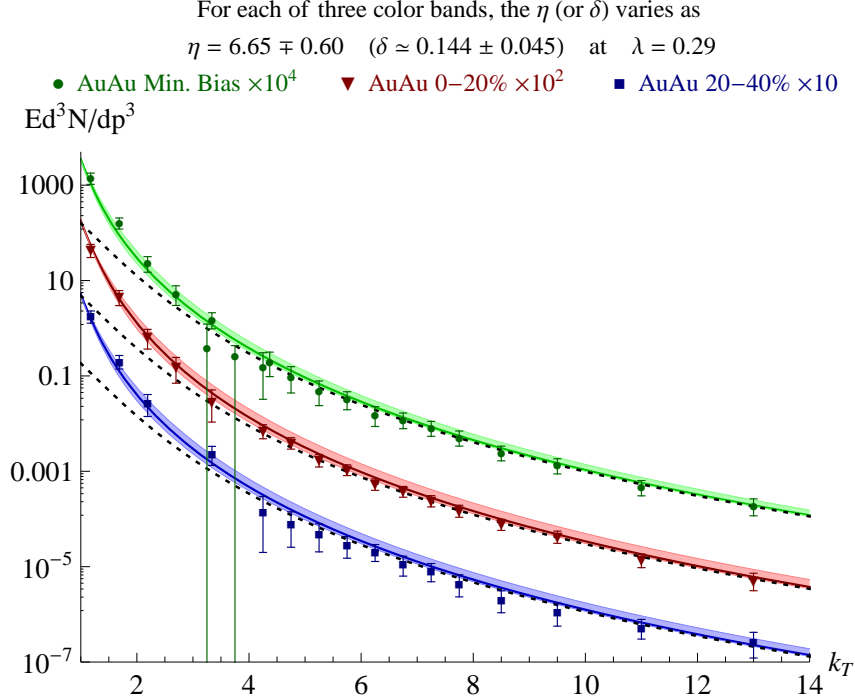


Figure 3: Comparison between the PHENIX photon data and the present model with  $\lambda = 0.29$  and varied values of  $\eta$  for three centrality bins. The black dashed curves represent the  $T_{AA}$ -scaled pp yield from Eq.(33), and the colorful bands represent full yield including also the Glasma contribution from Eq.(32) with the upper and lower boundary curves for each band corresponding to the results with the parameter  $\eta = 6.05$  and  $\eta = 7.25$ , respectively (see text for more details).

to indicate strong anisotropy between longitudinal and transverse scales in the Glasma evolution.

An issue we cannot address at present is the fact that the photon excess measured at PHENIX has reasonably large  $v_2$  [20]. Although we expect sizable flow to be developed in the Glasma, it remains an issue to see if this can be quantitatively resolved.

## 4.2 Di-leptons

Let's now consider the dilepton differential yield in both mass and transverse momentum  $k_T$ . Based on the results in the previous section, we take the phenomenological formula to be of the form

$$\frac{dN_{C \rightarrow DY}}{d^2k_T dy dM^2} = C_{ll} N_{part}^{2/3} \left( \frac{Q_{sat}}{M} \right)^{\eta'} \frac{e^{-k_T/\mu}}{\mu^2}, \quad (34)$$

The constant coefficient  $C_{ll} \sim \alpha^2 R_0'^2$  reflects the overall normalization to be fixed once and for all. In the above we have also introduced an exponential function for  $k_T$ -dependence with a width parameter

$\mu$ , which upon full integration over  $k_T$  will go back to the integrated yield in Eq.(26). While ideally the dilepton production from condensate would generate a delta function at  $k_T = 0$ , there however would be broadening in the pair  $k_T$  due to both the finite transverse size of the system and the transverse collective expansion, which is accounted for by the introduced exponential function. As before, we use the following for the saturation momentum

$$Q_{sat}^2(k_T/\sqrt{s}) = Q_0^2 \left( \frac{\sqrt{s} \times 10^{-3}}{k_T} \right)^\lambda e^{\lambda y}, \quad (35)$$

which now includes its evolution with the transverse momentum  $k_T$  as well as the rapidity  $y$ .

The dilepton data we aim to describe are the  $k_T$ -dependence of the dilepton yield at various given mass bins, as measured e.g. by PHENIX in [6] (see Fig. 37 there) for the  $k_T$ -spectra of  $e^+e^-$  pairs in  $Au + Au$  200 GeV minimal bias collisions in different mass bins. For a given mass bin  $[M_{min}, M_{max}]$ , we can integrate the differential yield to obtain the  $k_T$ -spectra:

$$\frac{dN_{C \rightarrow DY}}{2\pi k_T dk_T dy} = C_{ll} N_{part}^{2/3} Q_{sat}^{\eta'} \frac{e^{-k_T/\mu}}{\mu^2} \int_{M_{min}}^{M_{max}} \frac{2M}{M^{\eta'}} dM, \quad (36)$$

which eventually leads to

$$\begin{aligned} \frac{1}{(N_{part}/2)} \frac{dN_{C \rightarrow DY}}{2\pi k_T dk_T dy} &= \frac{4C_{ll}}{(2 - \eta')} N_{part}^{-1/3} \times (M_{max}^{2-\eta'} - M_{min}^{2-\eta'}) \\ &\times \frac{e^{-k_T/\mu}}{\mu^2} \times \left( Q_0^2 \left( \frac{\sqrt{s} \times 10^{-3}}{k_T} \right)^\lambda \right)^{\eta'/2}. \end{aligned} \quad (37)$$

In the above we've also incorporated Eq.(35). At this point it shall be emphasized that in our model the dilepton pairs generated from the Glasma shall have their mass bounded by the in-medium mass of gluons in the Glasma, and therefore our formula shall not be applied to too small values for the pair mass. Accordingly, we focus on comparison with data in a mass regime  $0.3 \text{ GeV} \leq M \leq 1 \text{ GeV}$ . Since the parameters  $\lambda$  and  $\eta'$  (determined by  $\delta$ ) are well constrained from the photon fitting, we will use those optimal values implied by photon data also for the dilepton fitting, i.e.  $\lambda = 0.29$  and  $\eta' = 4.73 \pm 0.20$  (corresponding to  $\delta = 0.144 \mp 0.045$ ).

We now present our fitting results for the PHENIX dilepton data in the Fig.4. For each bin of  $e^+e^-$  pair mass  $M \equiv m_{ee}$ , the dashed curves represent the background yield formed by contributions of the hadronic decay cocktail and charmed mesons. For the three higher mass bins relevant to the production from the Glasma, we also add on top of the background the additional contribution given by Eq. (37): the results for total yield are represented by the colorful bands where the upper and lower boundary curves for each band correspond to the results with the parameter  $\eta' = 4.93$  and  $\eta' = 4.53$ , respectively. For the  $k_T$  width we have found the optimal value  $\mu = 0.250 \text{ GeV}$  which would correspond to a "temperature"  $\sim 100 \text{ MeV}$  in thermal fits, i.e. rather "cold". The fitting quality has a relatively strong dependence on  $\mu$ . The optimal value for the overall normalization  $C_{ll}$  determined from such fitting is  $C_{ll} \approx 5.0 \times 10^{-6} f m^2$ . This coefficient  $C_{ll}$  is plausibly expected to be parametrically much smaller than the  $C_\gamma$  in the photon case as the former has one more power in its dependence on the electromagnetic coupling  $\alpha = 1/137$ .

The comparison for the mass region from  $300 \text{ MeV}/c^2$  to  $990 \text{ MeV}/c^2$  again shows nice agreement between data and model fitting results, and appears to suggest that the dilepton excess shown in

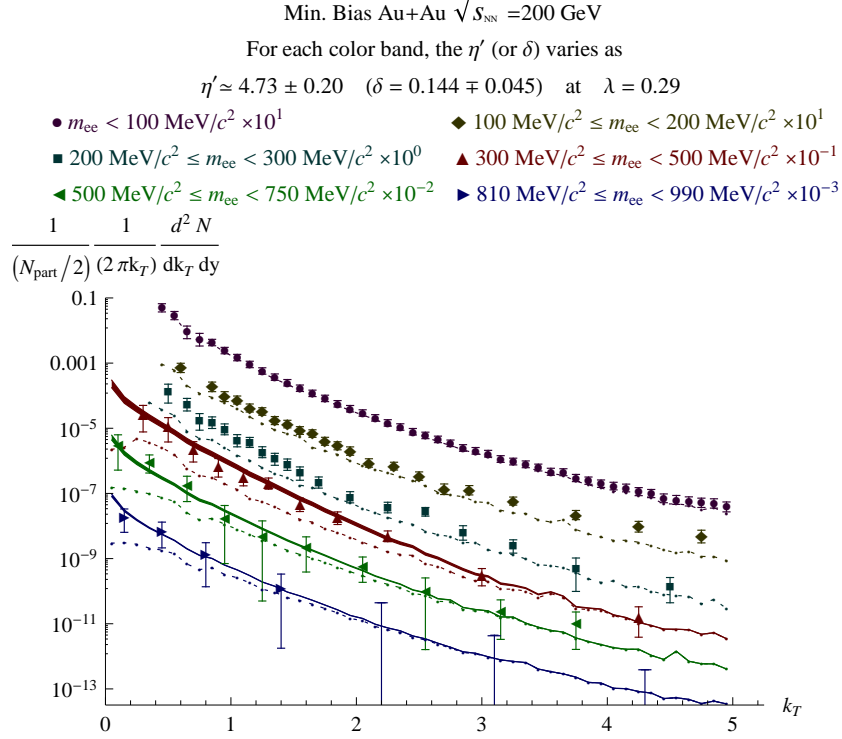


Figure 4: Comparison between the PHENIX photon data and the present model with parameters  $\lambda = 0.29$  and  $\eta' = 4.73 \pm 0.20$  for the three higher mass bins. The dashed curves represent the background contributions from hadronic cocktail and charmed mesons, and the colorful bands represent full yield including also the Glasma contribution from Eq.(37) with the upper and lower boundary curves for each narrow band corresponding to the results with the parameter  $\eta' = 4.93$  and  $\eta' = 4.53$ , respectively (see text for more details).

these PHENIX data for the small  $k_T$  regime, which is otherwise hard to explain, could be reasonably described by the Glasma contribution given by Eq. (37). The comparison also demonstrates that the PHENIX data for both photons and dileptons can be consistently described with the same parameter set  $\lambda = 0.29$  and  $\delta = 0.144 \pm 0.045$ . We have tested other choices of  $\lambda$  and  $\delta$  and found that the dilepton fitting results are less sensitive but nevertheless get worse gradually when deviating from the optimized regime as in the case of photons. As emphasized previously, the condensate production of dilepton pairs needs a better theoretical treatment. Provided our current crude estimate for such contribution, the dilepton results shall be considered mostly qualitative and suggestive.

We end by presenting our model results for a different observable of dilepton yield: the pair mass spectra for selected kinetic bins which can be obtained by integrating Eq. (34) over specific intervals

e.g.  $k_{T,min} \leq k_T \leq k_{T,max}$  and  $-Y_0 \leq y \leq Y_0$ . This leads to the following:

$$\begin{aligned} \frac{dN_{C \rightarrow DY}}{dM} &= 4\pi C_{ll} N_{part}^{2/3} \frac{\left(Q_0^2 (\sqrt{s} \times 10^{-3})^\lambda\right)^{\eta'/2}}{\mu^2} \times \\ &\times \left( \int_{k_{T,min}}^{k_{T,max}} k_T^{1-(\lambda\eta'/2)} e^{-k_T/\mu} dk_T \right) \left( \int_{-Y_0}^{Y_0} e^{(\lambda\eta'/2)y} dy \right). \end{aligned} \quad (38)$$

Specifically if one selects  $k_{T,min} = 0$  and  $k_{T,max} = 0.5 \text{ GeV}/c$ , the above Eq. (38) then becomes

$$\begin{aligned} \frac{dN_{C \rightarrow DY}}{dM} &= 4\pi C_{ll} N_{part}^{2/3} \frac{\left(Q_0^2 (\sqrt{s} \times 10^{-3})^\lambda\right)^{\eta'/2}}{\mu^2} \left( \frac{1}{M^{\eta'-1}} \right) \times \\ &\times \left( \left( \frac{1}{\mu} \right)^{-2+(\lambda\eta'/2)} \left[ \Gamma(2 - 0.5\lambda\eta') - \Gamma\left(2 - 0.5\lambda\eta', \frac{0.5}{\mu}\right) \right] \right) \left( \frac{4 \sinh[(\lambda\eta'/2)Y_0]}{\lambda\eta'} \right) \end{aligned} \quad (39)$$

This formula for the  $M$ -dependence of the dilepton yield at various  $k_T$  and  $y$  ranges can be appropriately tested when the corresponding spectra will be available after doing corrections to the PHENIX detector's acceptance (the un-corrected distributions are available though).

## 5 Summary and Conclusions

The conclusion of this paper is that the photons and dileptons data measured at PHENIX may be consistent with a scenario that assumes important electromagnetic production during the pre-equilibrium stage based on the Glasma hypothesis and the existence of a condensate. There are of course alternative explanations. We briefly outline below some of the places where alternative hypothesis may be viable or attractive and where further investigations would be desired.

- The steepness of the photon spectrum might simply be associated with a depletion of quarks relative to their equilibrium abundance. The relative abundance  $N_{quark}/N_{gluon} \sim \alpha_S$  is small in the initial stages of the Glasma expansion and this rises to be of the order one at the thermalization time. The quark number density therefore shall rise more rapidly than the gluon density at early times, which may result in a steeper photon spectrum than would be the case in the absence of such effect. This may be more a generic feature of the early time evolution rather than specific to our thermalization scenario.
- If the power law exponent associated with the photon spectrum is  $n$ , we would expect that the measured  $k_T$  arises from a typical energy scale of the Glasma of the order  $k_T \sim n E_{glasma}$ . More specifically, for photons of  $3 \text{ GeV}$  and  $n \sim 8$ , this would imply a typical scale of order  $400 \text{ MeV}$  in the Glasma. However, for momentum scales of order  $k_T \sim 1 \text{ GeV}$ , the scale would then be rather close to the transition temperature, and the Glasma description would surely break down. Note that for a steeper spectrum, the typical momentum scale is more sensitive to the lower momentum scale of the system — this may make it easier to generate flow for the photons, as we are weighting more at later times. But again such an effect may be more a generic feature associated with a steep spectrum due to the rapid rise of the quark density as already pointed out.

- The large flow seen in the PHENIX experiment may also rely on other enhancements associated with the Glasma. The Glasma has a typical transverse momentum scale large compared to the longitudinal, and the system is very strongly interacting at very early times. Nevertheless, it takes time to build up the collective flow, and at the moment it is not yet clear whether enough flow could be generated early on in the Glasma. This issue will be investigated in future works.
- The geometric scaling of the photon spectra provides very strong evidence for the saturation nature of the initial conditions for the Glasma. However this scaling may also be preserved by hydrodynamic computations with saturation-type initial conditions. The geometric scaling is moreover a generic feature of any interaction that would survive from initial conditions to hadronization. While the centrality dependence of photon spectra provides a very sensitive test of the geometric scaling, it may not be unique to the present Glasma model.
- The condensate formation in the Glasma is very speculative and at present not well established from theoretical principles. It could be that there are other condensates which can decay at late times and generate the low-mass low-momentum di-lepton excess. The over-occupation of the initial conditions for the Glasma will induce a condensate but as time evolves, this condensate might change its character or new condensates might form and evaporate. That said, the generic signature of small transverse momentum of the excess di-lepton pairs relative to their mass could be a strong indication of certain condensate formation.
- At present a reliable computation of the rate of di-lepton production through quark loops is still lacking and will be explored in future works. It could be that the overall rate may turn out to be too small to explain the PHENIX results. It also may be that the di-leptons are formed at late times in a hadronic stage, where the nature of the condensate and its decay mechanism might be quite different from the condensate in the Glasma.
- Most importantly, the present data on di-leptons are controversial due to the quite different results from PHENIX and STAR measurements. The data in its present state appear too sparse to draw any strong conclusion from theoretical modeling. It is desirable to have future high-precision data that can clearly establish whether the origin of the excess is associated with small transverse momenta or not. It is also essential to have more data on the mass dependence of the effect in various transverse momentum bins for different centrality bins. If it would eventually be confirmed that there is indeed a large excess of di-leptons arising just at small  $p_T$ , for the reasons stated above, this would be a very important scientific discovery.

## Acknowledgements

The research of T. K. Hemmick and V. Khachatryan is supported under DOE Contract No. DE-FG02-96ER40988. A. Leonidov acknowledges support from the RFBR grant 12-02-91504-CERN and RAS LHC program. The research of J. Liao and L. McLerran is supported under DOE Contract No. DE-AC02-98CH10886. L. McLerran thanks the Theoretical Physics Institute of the University of Heidelberg where this work was in part developed. He is supported there as a Hans Jensen Professor of Theoretical Physics. J. Liao is grateful to RIKEN BNL Research Center for partial support.



## References

- [1] E. V. Shuryak, Phys. Lett. **B78**, 150 (1978).
- [2] L. D. McLerran, T. Toimela, Phys. Rev. **D31**, 545 (1985).
- [3] B. Sinha, Phys. Lett. B **128**, 91 (1983).
- [4] D. K. Srivastava, B. Sinha, M. Gyulassy and X. -N. Wang, Phys. Lett. B **276**, 285 (1992).
- [5] A. Adare *et al.* [ PHENIX Collaboration ], Phys. Rev. Lett. **104**, 132301 (2010). [arXiv:0804.4168 [nucl-ex]].
- [6] A. Adare *et al.* [ PHENIX Collaboration ], Phys. Rev. **C81**, 034911 (2010). [arXiv:0912.0244 [nucl-ex]].
- [7] A. Adare *et al.* [ PHENIX Collaboration ], arXiv:1105.4126 [nucl-ex].
- [8] J. -P. Blaizot, F. Gelis, J. Liao, L. McLerran, R. Venugopalan, Nucl. Phys. **A873**, 68-80 (2012). [arXiv:1107.5296[hep-ph]].
- [9] A. Kovner, L. D. McLerran, H. Weigert, Phys. Rev. **D52**, 6231-6237 (1995). [hep-ph/9502289].
- [10] A. Kovner, L. D. McLerran, H. Weigert, Phys. Rev. **D52**, 3809-3814 (1995). [hep-ph/9505320].
- [11] A. Krasnitz, R. Venugopalan, Phys. Rev. Lett. **84**, 4309-4312 (2000). [hep-ph/9909203].
- [12] T. Lappi, L. McLerran, Nucl. Phys. **A772**, 200-212 (2006). [hep-ph/0602189].
- [13] L. D. McLerran, R. Venugopalan, Phys. Rev. **D49**, 2233-2241 (1994). [arXiv:hep-ph/9309289 [hep-ph]].
- [14] G. Wang [STAR Collaboration], *Proceedings of 7'th International Conference on the Critical Point and the Onset of Deconfinement*, Wuhan, China, Nov 7-11 (2011). [arXiv:1201.4202 [nucl-ex]].
- [15] J. Liao, E. Shuryak, Phys. Rev. Lett. **101**, 162302 (2008); Phys. Rev. **C75**, 054907 (2007); Nucl. Phys. **A775**, 224-234 (2006).
- [16] D. K. Srivastava, Pramana **57**, 235-249 (2001).
- [17] L. McLerran and M. Praszalowicz, Acta Phys. Polon. B **41** (2010) 1917, arXiv:1006.4293 [hep-ph].
- [18] D. Kharzeev, E. Levin and M. Nardi, Nucl. Phys. A **747** (2005) 609, [arXiv:hep-ph/0408050].
- [19] D. Kharzeev and M. Nardi, Phys. Lett. B **507** (2001) 121, [arXiv:nucl-th/0012025].
- [20] E. Kistenev [PHENIX Collaboration], J. Phys. **G 38**, 124137 (2011).